Available online at www.CivileJournal.org

Civil Engineering Journal

(E-ISSN: 2476-3055; ISSN: 2676-6957)

Vol. 8, No. 09, September, 2022

Efficiency of Friction Pendulum Bearings in Vertically Irregular Structures Subjected to Various Types of Earthquakes

Jamal Ghazi Al Adwan [1], Salam Al Kasassbeh [1], Jafar Al Thawabteh [1], Bilal Yasin [2], Yazan Alzubi [1*]

[1] *Civil Engineering Department, Faculty of Engineering Technology, Al-Balqa Applied University, Amman, Jordan.*

[2] *Civil Engineering Department, Faculty of Engineering, Al al-Bayt University, 25113 Mafraq, Jordan.*

Received 21 June 2022; Revised 11 August 2022; Accepted 27 August 2022; Published 01 September 2022

Abstract

The attention towards seismic mitigation using passive control systems has increased significantly over the last few decades to reduce earthquake demands and achieve the required performance objectives. Nowadays, friction pendulum bearings have proven efficient in mitigating regular RC structures subjected to a wide range of earthquakes. Nonetheless, limited studies were dedicated to investigating the performance and efficiency of this type of isolation system utilized in RC structures with various types of vertical irregularities. Besides, comprehensive parametric assessments that investigate the behavior of structures supported on friction pendulum bearings subjected to pulse-like and non-pulse-like earthquakes are scarce. Thus, this study aims to assess the behavior of RC frames equipped with friction pendulum isolators under different types of earthquakes. In the context of the paper, three types of vertical irregularities, known as soft-story, heavy-story, and stepped structures, will be modeled and investigated. Moreover, the outcomes of these buildings will be benchmarked to a regular model to illustrate the efficiency of the selected isolation systems. Furthermore, the performance of the base-isolated buildings with friction pendulum isolators subjected to pulse-like and non-pulse-like earthquakes will be reported. In general, the study results have shown that pulse-like earthquakes exhibited higher values than non-pulse-like earthquakes for the different responses of the structures at the periods of 2.5 and 3 and the damping ratios of 15%, 20%, and 25%.

Keywords: Reinforced Concrete; Low-Rise Structure; Friction Pendulum Isolators; Pulse-Like and Non-Pulse-Like Earthquake; Vertical Irregularity; Nonlinear Response History Analysis.

1. Introduction

The effects of strong earthquakes can result in catastrophic damage to structural and non-structural components of RC structures, particularly in the case of irregular RC structures [1-3]. In some cases, irregularity can result from surpassing the boundaries indicated in seismic design codes due to a structure's utility or design demands [4]. Generally, incorporating a seismic control system into an RC structure is necessary to protect the structure under severely dangerous earthquakes [5]. Implementing a base isolation system in the RC structure is considered one of the methods to protect the structure during earthquakes by minimizing the responses, including acceleration and displacement, via maximizing the structure's natural period [6, 7].

Nonetheless, near-fault earthquakes with a long-period pulse can diminish the system's capability via significant replacement of the isolation bearing, yielding instability in the base-isolated structure [8, 9]. Therefore, many studies have recently focused on investigating the efficiency of base-isolated structures subjected to pulse-like and non-pulse-

* Corresponding author: yazan.alzubi@bau.edu.jo

http://dx.doi.org/10.28991/CEJ-2022-08-09-05

like earthquakes [10-12]. Mazza and Mazza [11] investigated the performance of friction pendulum isolators equipped with vertical and horizontal irregular RC structures. In addition, Mazza [13] evaluated the seismic performance of RC structures supported on elastomeric isolators during ground motions. Moreover, another study was conducted to examine the irregularity in stiffness (soft story) by means of incorporating different base isolators into soft story structures [14]. However, no study was conducted to investigate the efficiency of the friction pendulum isolator utilized with different vertical irregular RC structures subjected to pulse-like and non-pulse-like earthquakes.

Thus, this study is intended to examine the efficiency of friction pendulum isolators implemented with different types of vertical irregular RC structures subjected to pulse-like and non-pulse-like earthquakes. Consequently, investigation regarding the effect of the heavy story, soft story, and stepped frames on the efficiency of the friction pendulum during pulse-like and non-pulse-like earthquakes. Therefore, this paper is dedicated to investigating the seismic performance of low-rise irregular RC structures equipped with friction pendulum isolators under pulse-like and non-pulse-like earthquakes. In order to do so, an investigation of the seismic behavior of irregular RC structures under pulse-like and non-pulse-like ground motions will be performed using finite element analysis. Furthermore, the friction pendulum isolator's efficiency will be examined by investigating the seismic performance of irregular base-isolated RC frames under pulse-like and non-pulse-like earthquakes. Hence, this study is devoted to bridging the gap in the literature and investigating the performance of base-isolated structures utilized with friction pendulum isolators during pulse-like and non-pulse-like earthquakes, particularly in earthquake-prone countries. Finally, the effect of irregularity type on the friction pendulum isolator in RC structures subjected to pulse-like and non-pulse-like earthquakes will be evaluated.

2. Materials and Methods

Seismic performance assessment of base-isolated structures is critical regarding friction pendulum bearings' safety, efficiency, and feasibility. In this study, the efficiency of vertically irregular RC structures equipped with friction pendulum bearings and subjected to pulse-like and non-pulse-like ground motions will be investigated numerically using the nonlinear time history analysis approach by focusing on the effect of the irregularity type on the change in response. The research methodology of this investigation is indicated in Figure 1. In general, the research will first define the case studies and select the earthquake types. Then, nonlinear response history analyses will be conducted considering isolator and superstructure nonlinearity. Finally, the results will be interpreted and benchmarked to a regular base-isolated building to illustrate the impact of the type of irregularity on the efficacy of the isolator in controlling the building's response.

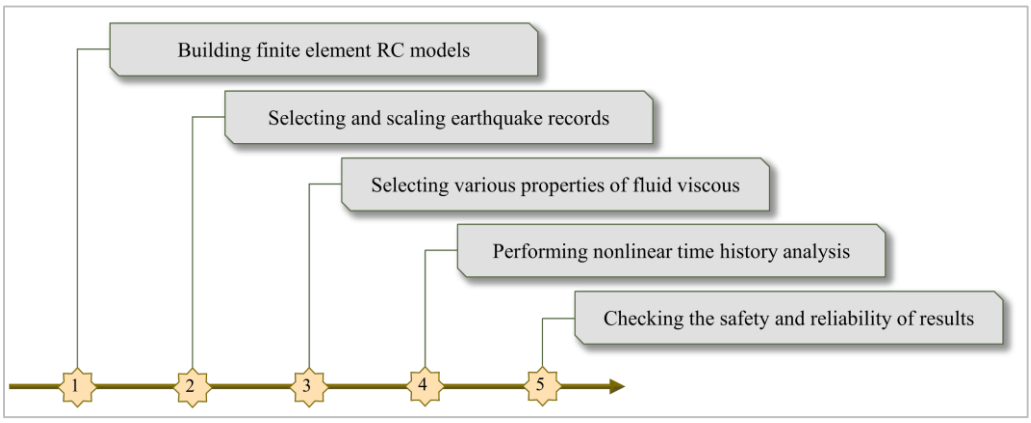

Figure 1. Research methodology flowchart

The different aforementioned vertical irregularity types, which are irregularity in mass (heavy story), irregularity in stiffness (soft story), and irregularity in geometry (stepped structure), will be described in this section of the study. The first vertical irregularity discussed in the study is a heavy story. This irregularity emerges from the mass increment of one story by approximately 150% compared to the adjacent story [15]. Mass irregularity can occur in the structures' low, middle, and high stories. In this study, 1.66 times increment in the weight of the second story was developed to produce mass irregularity in that story. The second irregularity considered is a soft story, which is by far the most prevalent vertical irregularity that can be yielded due to a decrease in the stiffness of one story regarding the rest of the stories. The influence of a soft story with respect to the displacement and story drift in the structure is akin to a heavy story case [16]. This irregularity usually can be developed on the structure's first floor and can be noticed in cases such as open floors and double height first soft stories. Double height first soft story case results from the flexibility (lower stiffness) of the columns in the first story in regards to the rest of the columns in the structure due to partial or total vacancies in the walls of the first story or due to relative increment in the height of the first story compared to the rest of the stories. The soft story is considered one of the most dangerous and disastrous vertical irregularities due to the flexible story's

absorption of the high input of energy leading to the development of large relative displacement between both ends of that story (inter-story drift) in contrast to the rigid upper stories' absorption of the rest of the distributed energy. Accordingly, damage to the structural elements or a total collapse of the structure can occur due to a discontinuity in stiffness between soft and rigid floors. The last vertical irregularity to be described in this section is the irregularity in geometry (stepped structure) which emerges from the reduction in geometry (lateral dimension) of the structure regarding the height [1]. This irregularity is developed as a result of an increment in the horizontal dimensions of the structure of approximately 130% with respect to the adjacent story [17]. As this irregularity develops, a sudden reduction in story area compared to the structure's height, yielding a decrease in mass, strength, and stiffness, is followed [1]. The danger of this irregularity stems from the vulnerability of stepped structures during earthquakes leading to instability where the story drift and displacement increase [18].

The base isolation system (friction pendulum isolator) was incorporated with these structures and examined their seismic performance. In order to study the irregularity impact on the efficiency and behavior of several friction pendulum isolators, the regular model will be set as the reference. The regular building is three bays and three stories of 3 m each. Three types of irregularities are selected, which are soft, heavy, and stepped structures. The soft story is defined by increasing the regular building's first story by 1.5 m. On the other hand, the heavy story is designed by increasing the load of the third story by 50%. Moreover, the stepped structure is achieved by removing one column and beam from the corner of the roof. The column (0.4 m by 0.4 m) and beam (0.4 m by 0.5 m) sections were made constant for all structures.

The friction pendulum isolator comprises the base plate, spherical concave dish, and articulated slider, which includes ductile iron with polytetrafluorethylene (PTFE) material, as illustrated in Figure 2. The displacement of the spherical concave dish occurs horizontally in relation to the base plate and articulated slider. Accordingly, the friction isolator's friction resistance and energy dissipation resulting from the friction between stainless steel and PTFE material. Moreover, the restoring force results from the radius of curvature of the spherical concave dish. Figure 3 shows the friction pendulum isolator's force displacement and bi-linear model. The following properties of the friction pendulum were computed to model the isolator. The bearing pressure, peak velocity, and material of the friction isolator govern the values of μ, which range from 0.07 to 0.18 for un-lubricated Teflon material [19, 20]. In this study, the efficiency of the friction pendulum isolator was investigated for two cases of natural periods of 2.5 seconds and 3 seconds as well as for three cases of damping ratios of 15%, 20%, and 25%. These values represent typical scenarios for the case of low-rise RC structures.

$$Q_d = \mu W \quad (1)$$

$$K_d = \frac{W}{r} \quad (2)$$

$$T_d = 2\pi\sqrt{\frac{r}{g}} \quad (3)$$

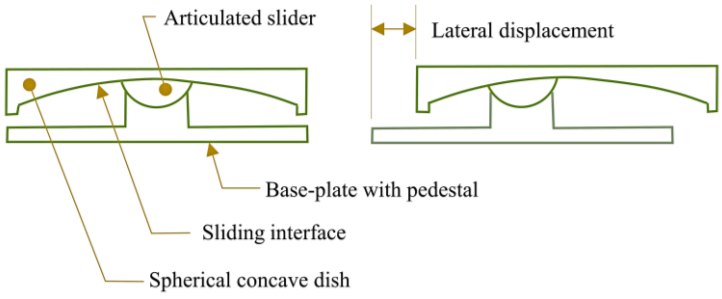

Figure 2. Components of FP

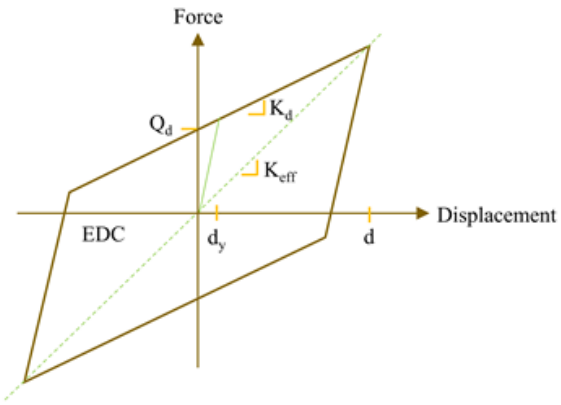

Figure 3. Bilinear horizontal force-displacement of friction pendulum isolator

The effective stiffness described in ACI 318-19 code was used to simulate the column and beam sections' stiffness properties via the linear elastic approach, where finite element software (SAP2000) was performed to model the two-degree freedom (2 DOF) system for evaluating the inelastic seismic response of the structure utilized with base isolation system [21]. The equivalent lateral force approach described in ASCE/SEI 7-16 code was used to evaluate the adequacy of the retrofitting [17].

The nonlinear modeling of all structures was conducted using the NIST GCR 17-917-46v3 guideline [22]. Mander et al. [23] model was performed to represent the fiber section of the concrete model's unconfined and confined compressive stress-strain behavior. Park and Paulay [24] approach was to define the rebars' stress-strain behavior. The unconfined concrete cover, confined concrete core, and rebars represent the three fiber parts of the structural elements defined in this study, similar to Kalantari and Roohbakhsh [25]. In order to simulate the nonlinear behavior of the structural components, a concentrated hinge model was used. SAP2000 [26] was used to conduct a nonlinear time history analysis (direct integration approach). The first fundamental mode period, 2.5%, is multiplied by the damping ratio at periods of 1.5 and 0.25, representing the typical damping in the superstructure.

A suit of 18 real pulse-like and non-pulse-like earthquake records was chosen to perform this study using Pacific Earthquake Engineering Research Center (PEER) (Table 1). Indeed, the PEER website tool was used to scale the 18 earthquakes over the range of period from 0 to 5 seconds, as shown in Figure 4, to calculate a single scale factor for each earthquake that minimizes the mean square error between the mean and the scaled earthquake records' target spectrums. In order to account for the influence of the structure's free vibration response, 15 seconds of zeroes were added at the end of each earthquake record [27-30].

Table 1. Selected earthquake records

Year	Earthquake Name	Type	Magnitude (Mw)	Vs30 (m/s)	Fault Distance (km)	PGA (g)	PGV (m/s)
1940	Imperial Valley-02	Non-Pulse	6.95	213.44	6.09	0.281	0.310
1971	San Fernando	Non-Pulse	6.61	459.37	108.01	0.043	0.037
1984	Morgan Hill	Non-Pulse	6.19	488.77	3.26	0.423	0.254
1989	Loma Prieta	Non-Pulse	6.93	462.24	3.85	0.645	0.560
1994	Northridge-01	Non-Pulse	6.69	416.58	22.5	0.185	0.241
1999	Chi-Chi Taiwan	Non-Pulse	7.62	443.04	8.2	0.447	0.402
1999	Chi-Chi Taiwan	Non-Pulse	7.62	459.34	7.4	0.228	0.598
2000	Tottori Japan	Non-Pulse	6.61	420.2	8.83	0.630	0.399
2004	Parkfield-02 CA	Non-Pulse	6	450.61	6.3	0.209	0.126
1979	Imperial Valley-06	Pulse	6.53	242.05	0.65	0.287	0.353
1979	Imperial Valley-06	Pulse	6.53	264.57	0.07	0.317	0.730
1989	Loma Prieta	Pulse	6.93	380.89	8.5	0.514	0.416
1992	Cape Mendocino	Pulse	7.01	422.17	8.18	0.591	0.496
1994	Northridge-01	Pulse	6.69	525.79	5.43	0.571	0.762
1994	Northridge-01	Pulse	6.69	285.93	5.48	0.419	1.182
1999	Chi-Chi Taiwan	Pulse	7.62	462.1	8.27	0.174	0.515
2003	Bam Iran	Pulse	6.6	487.4	1.7	0.808	1.241
2010	Darfield New Zealand	Pulse	7	295.74	8.46	0.257	0.394

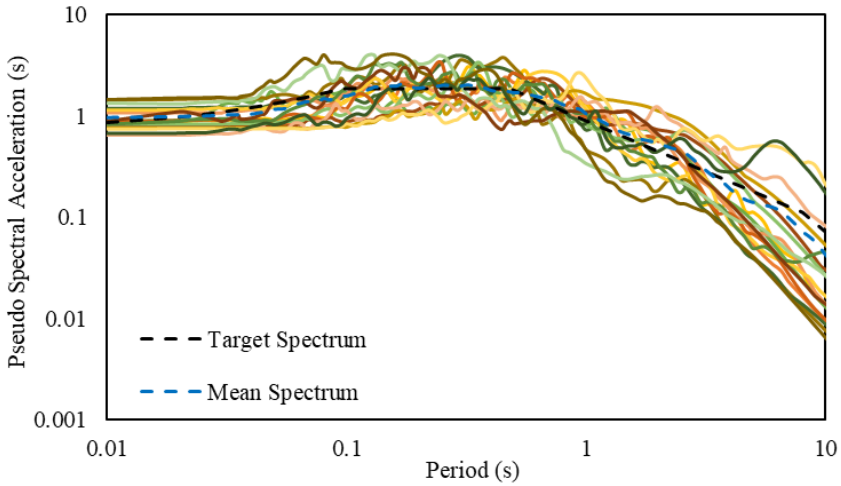

Figure 4. Targeted spectrum versus the mean one for the selected ground motion records

3. Results and Discussions

The use of a base isolation system at different periods and damping ratios was performed to investigate the seismic behavior and the effect of pulse-like and non-pulse-like earthquakes on the efficiency of the friction pendulum isolator. The calculation of normalized base shear was done using Equation 4 by dividing the base shear values for each irregularity type at each damping ratio by the base shear values of the bare structure model. Figure 5 represents the normalized base shear of the selected earthquake records. In general, the soft story case was observed to express the highest base shear values at all tested periods and damping ratios, where the combination of 2.5 seconds period and a damping ratio of 25% was observed to mark the highest base shear value. On the other hand, the stepped structure case exhibited the lowest base shear values at all tested periods and damping ratios, where the combination of 3 seconds period and damping ratios of 20% and 25% were recorded to mark the lowest base shear value. The influence of increasing the period from 2.5 to 3 seconds reflected a drastic reduction in the base shear values compared to the effect of increasing the damping ratio from 15% to 25%. Lastly, the combination of 3 seconds period and a damping ratio of 25% showed the lowest base shear results among all combinations.

$$Normalized\ peak\ response = \frac{response\ of\ irregular\ base-isolation\ model\ at\ specific\ damping\ ratio\ and\ period}{response\ of\ regular\ structurs\ model\ at\ the\ same\ damping\ ratio\ and\ period} \quad (4)$$

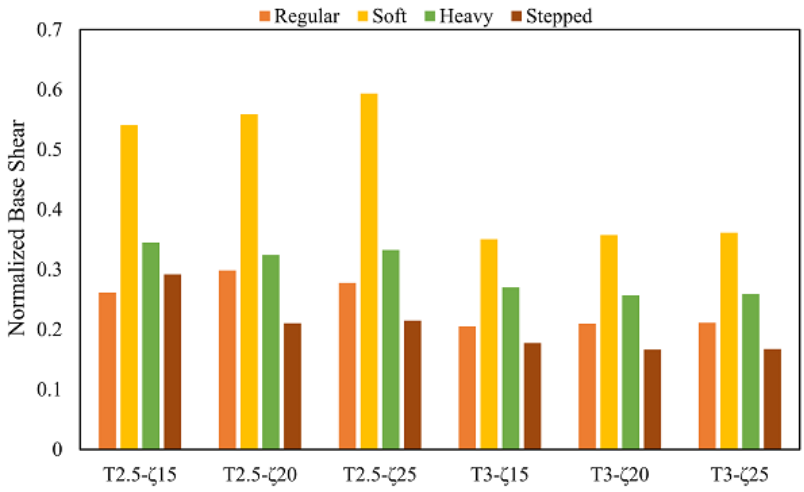

Figure 5. Normalized base shear of the investigated structures

Soft story irregularity reflected the highest normalized base shear results in both pulse-like and non-pulse-like earthquakes, as illustrated in Figure 6. The severity of soft story irregularity arises from the increase in the structure period as a result of the minimization of stiffness on the first floor, which diminishes the efficiency and performance of the isolator in contrast to the rest of the vertical irregularities [31, 32]. The lowest normalized base shear results for pulse-like and non-pulse-like earthquakes were seen as stepped structure models. Generally, the impact of pulse-like earthquakes exhibited much higher base shear results and hence more dangerous behavior than non-pulse-like earthquakes.

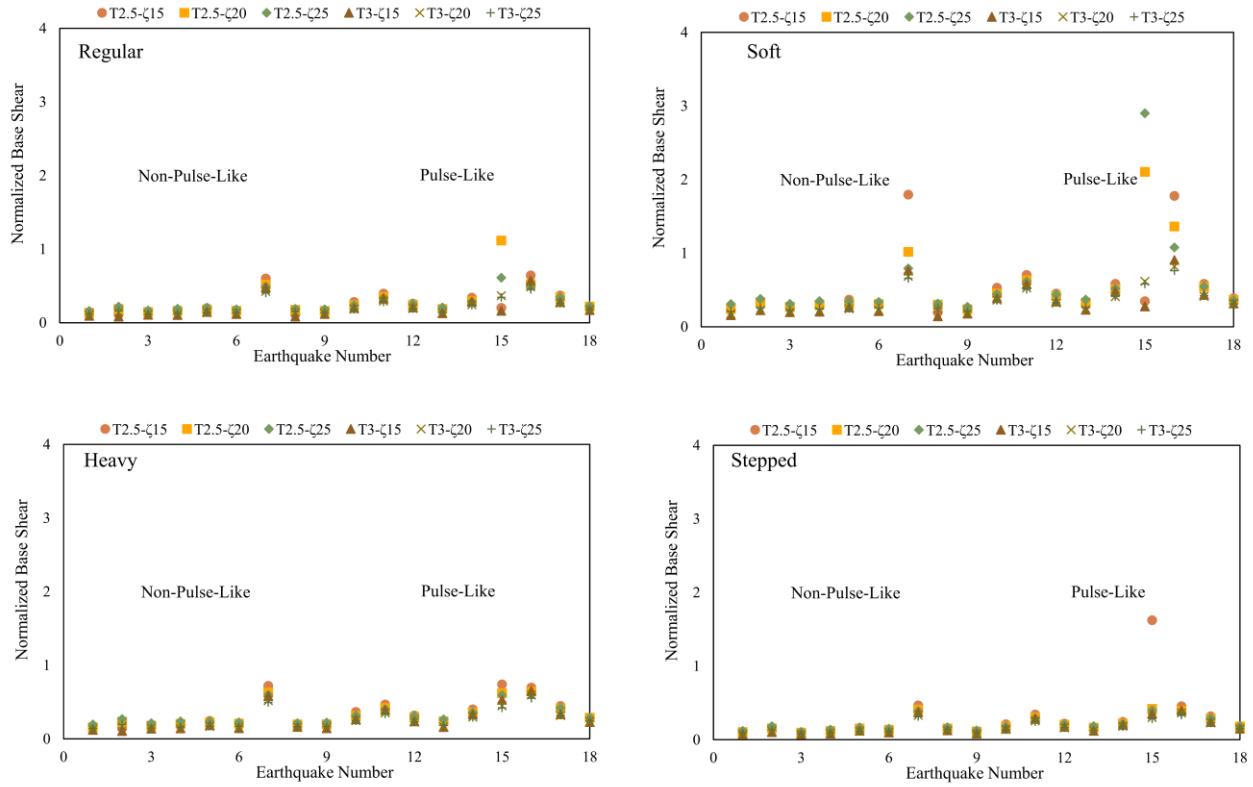

Figure 6. Influence of the pulse-like and non-pulse-like earthquakes on the normalized base shear of the selected earthquakes for (a) regular, (b) soft, (c) heavy, (d) stepped

The dashed line represents the normalized base shear where the base shear of the soft structure irregularity is divided by the base shear of the regular model. The bare structure represents the bare structure of each structure type, whereas the bare structure in the soft case represents the bare structure of soft irregularity. The effect of the base isolator on the behavior of irregularity type is illustrated in Figure 7, where the friction pendulum isolator exhibited improvement in the base shear response of the base-isolated structures (in the case of soft and heavy irregularities) since the base shear response was observed to surpass the dashed line.

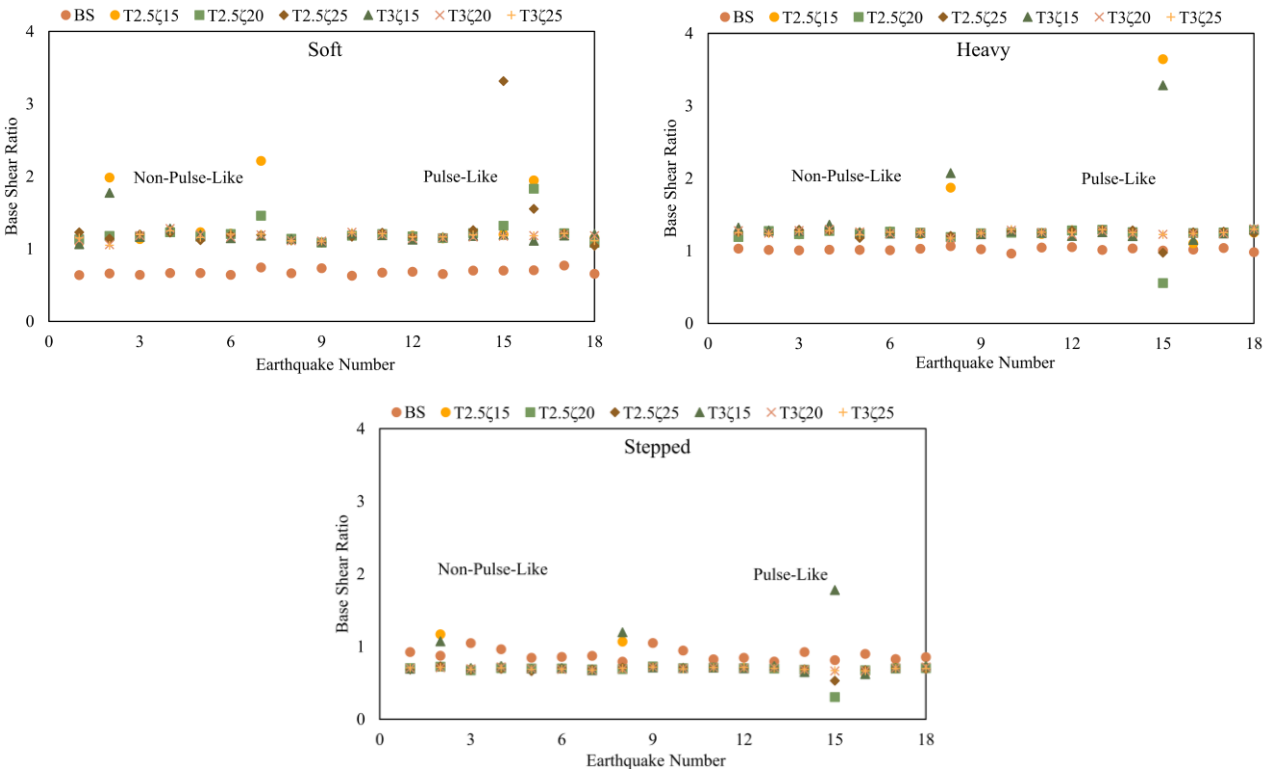

Figure 7. Base shear ratio of the selected earthquakes for irregular structures (a) soft, (b) heavy, (c) stepped

The normalized values of the roof displacement of the selected earthquake records are shown in Figure 8. The highest results of normalized roof displacement were for stepped structure irregularity, where the highest value was seen at the combination of 3 seconds period and a damping ratio of 15%. On the contrary, soft story irregularity displayed the least roof displacement results, where the least value was marked at the combination of 2.5 seconds period and a damping ratio of 25%. The period change from 2.5 to seconds resulted in a considerable increase in the roof displacement with respect to changing the damping ratio from 15% to 25%.

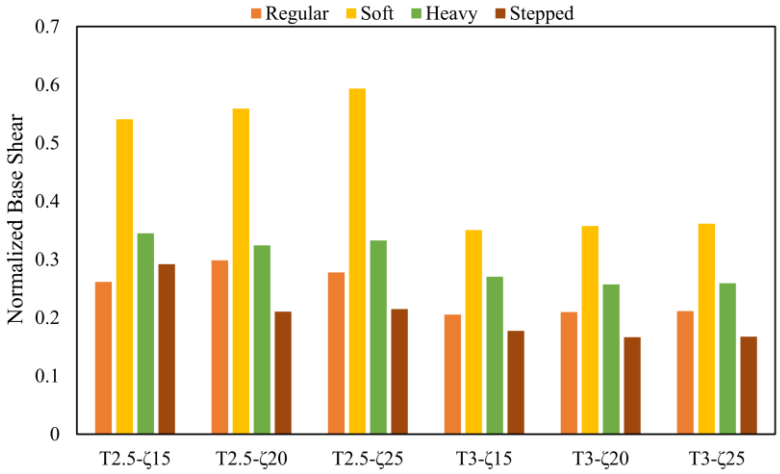

Figure 8. Normalized roof displacement of the investigated structures

Stepped structure irregularity represents the highest normalized roof displacement results for both pulse-like and non-pulse-like earthquakes, as shown in Figure 9. However, soft structure irregularity exhibited the lowest roof displacement results for pulse-like and non-pulse-like earthquakes. A similar influence of the irregularity was previously mentioned by Chen and Xiong [30]. Pulse-like earthquakes reflected a much stronger and more severe influence on the efficiency of friction pendulum isolator regarding non-pulse-like earthquakes.

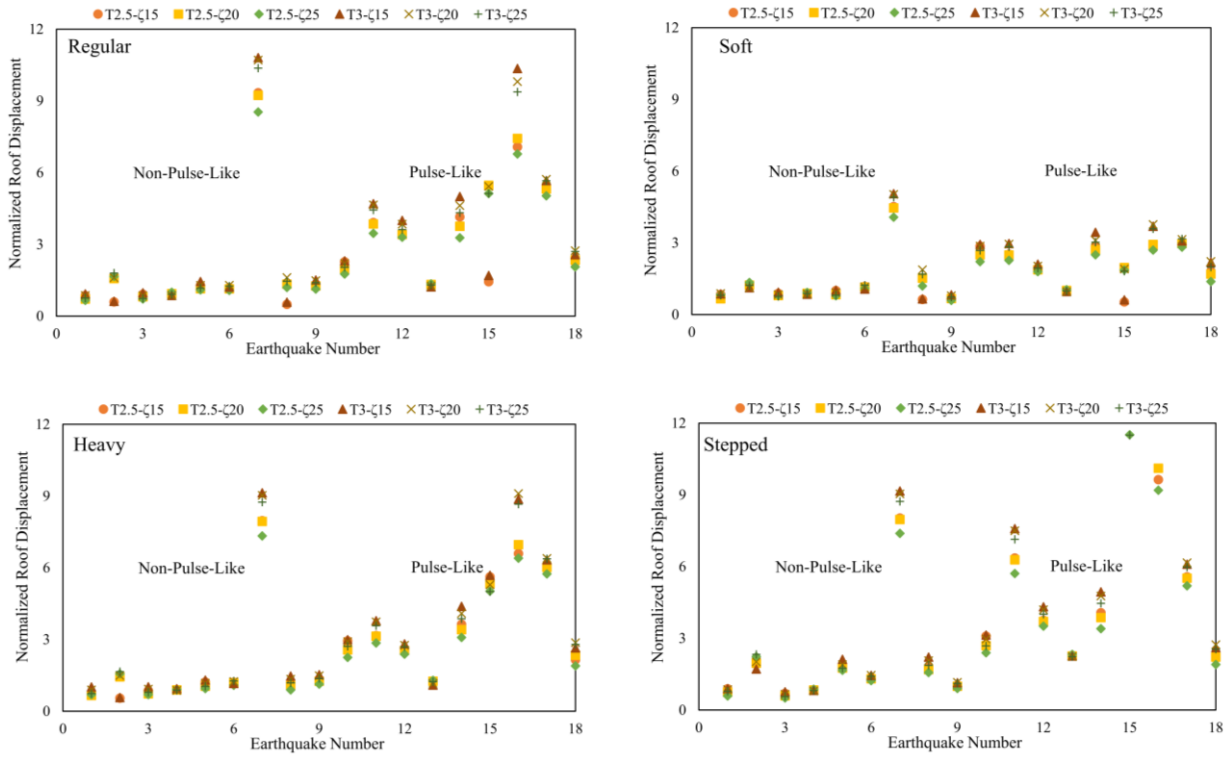

Figure 9. Normalized roof displacement of the selected earthquakes for (a) regular, (b) soft, (c) heavy, (d) stepped

The influence of roof displacement on the behavior of irregularity type is shown in Figure 10, where the friction pendulum isolator enhanced the roof displacement response of the base-isolated structures. However, the efficiency of the friction isolator in the case of the soft story is observed to be the least, which is in accordance with Figures 8 and 9. This can be seen where the bare structure's roof displacement was higher than the corresponding values of the base-isolated soft structure under all combinations of periods and damping ratios.

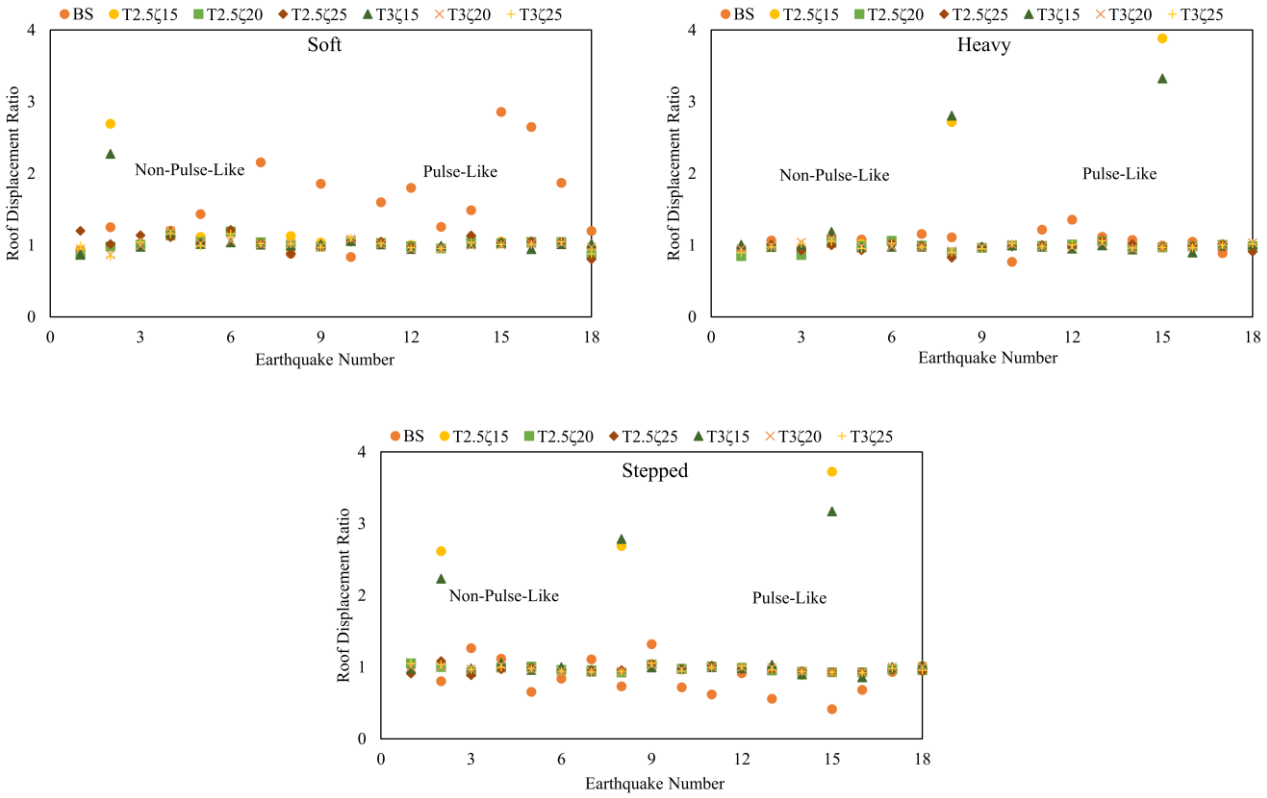

Figure 10. Roof displacement ratio of the selected earthquakes for irregular structures (a) soft, (b) heavy, (c) stepped

Soft case irregularity possessed the highest normalized roof acceleration results for the selected earthquake records as represented in Figure 11, where the highest value was observed at the combination of 2.5 seconds period and damping ratio of 25%, which is in accordance with the findings with other studies such as Gosh and Debbarma [18] where it was concluded that soft story is the most severe vertical irregularity. Conversely, the lowest roof acceleration result was seen in the stepped structure, where the lowest value was recorded at the combination of 3 seconds and a damping ratio of 15%. The roof acceleration response at the period of 2.5 seconds reflected the highest results in comparison to the period of 3 seconds in all cases of damping ratios. Furthermore, the 25% damping ratio showed the highest roof acceleration result between the different damping ratios for the two cases of 2.5- and 3-seconds periods. Finally, the roof acceleration response at the combination of 2.5 seconds period and a damping ratio of 25% exhibited the highest results among all combinations for the four cases of the investigated structures. Similarly, the roof acceleration response at the combination of 3 seconds period and damping ratio of 15% represented the least results among all combinations for the four cases of the investigated structures.

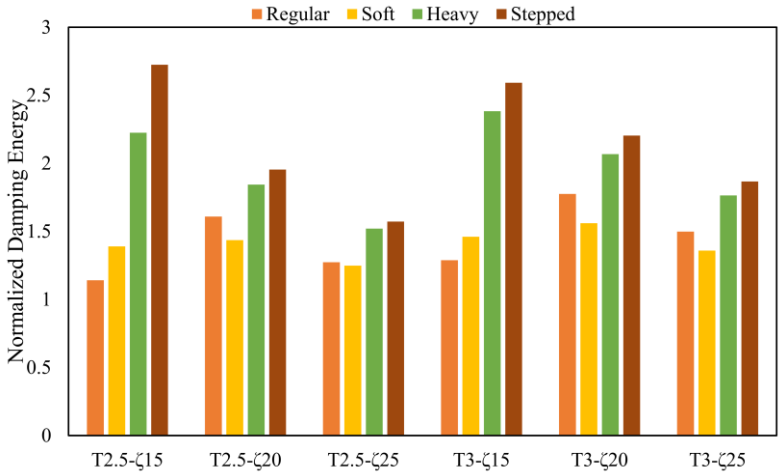

Figure 11. Normalized roof accelerations of the investigated structures

Normalized roof acceleration response was observed to reflect the highest results for pulse-like and non-pulse-like earthquakes, as shown in Figure 12. Nonetheless, the stepped structure showed the lowest roof acceleration results for both pulse-like and non-pulse-like earthquakes. In general, the results of pulse-like earthquakes were quietly comparable to those of non-pulse-like earthquakes for roof acceleration response.

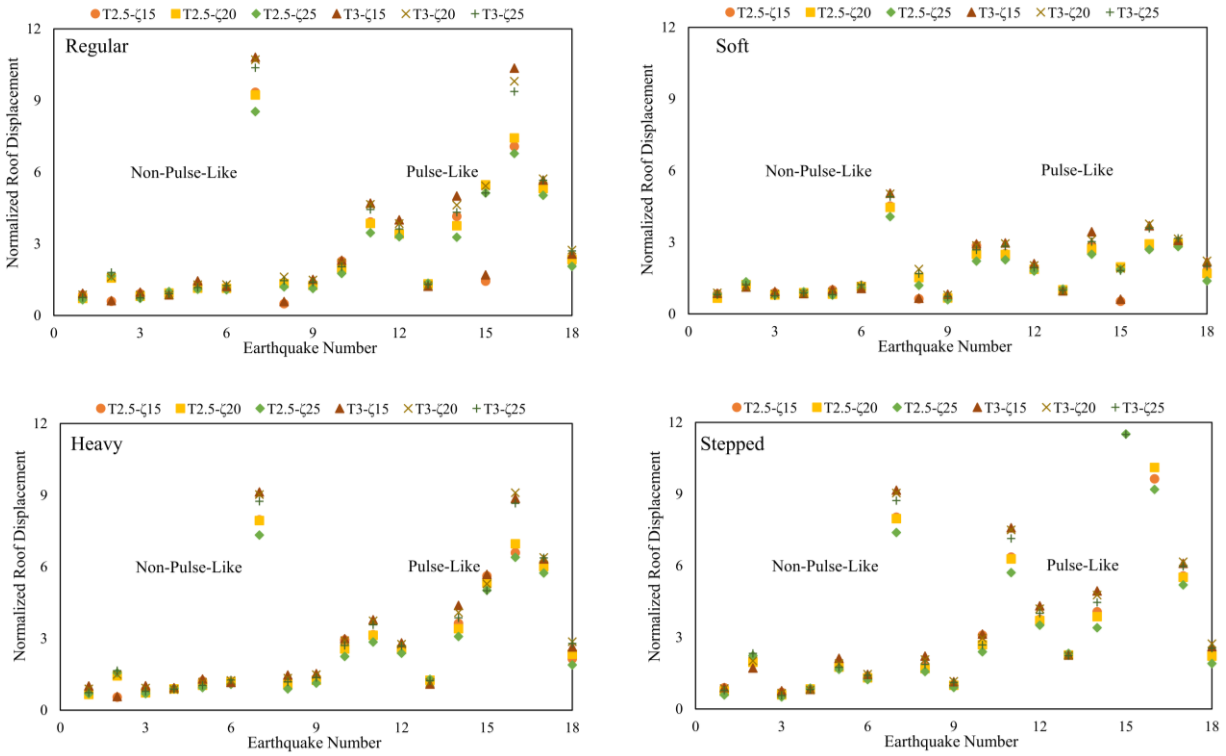

Figure 12. Normalized roof acceleration of the selected earthquakes for (a) regular, (b) soft, (c) heavy, (d) stepped

The impact of the base isolation system on the behavior of irregularity type is represented in Figure 13. The friction pendulum isolator showed superior performance in terms of roof acceleration of the base-isolated structures. Nonetheless, stepped structure irregularity experienced the lowest performance of friction pendulum isolator since the response of the bare structure was larger than that of base-isolated stepped ones which is consistent with Figures 11 and 12.

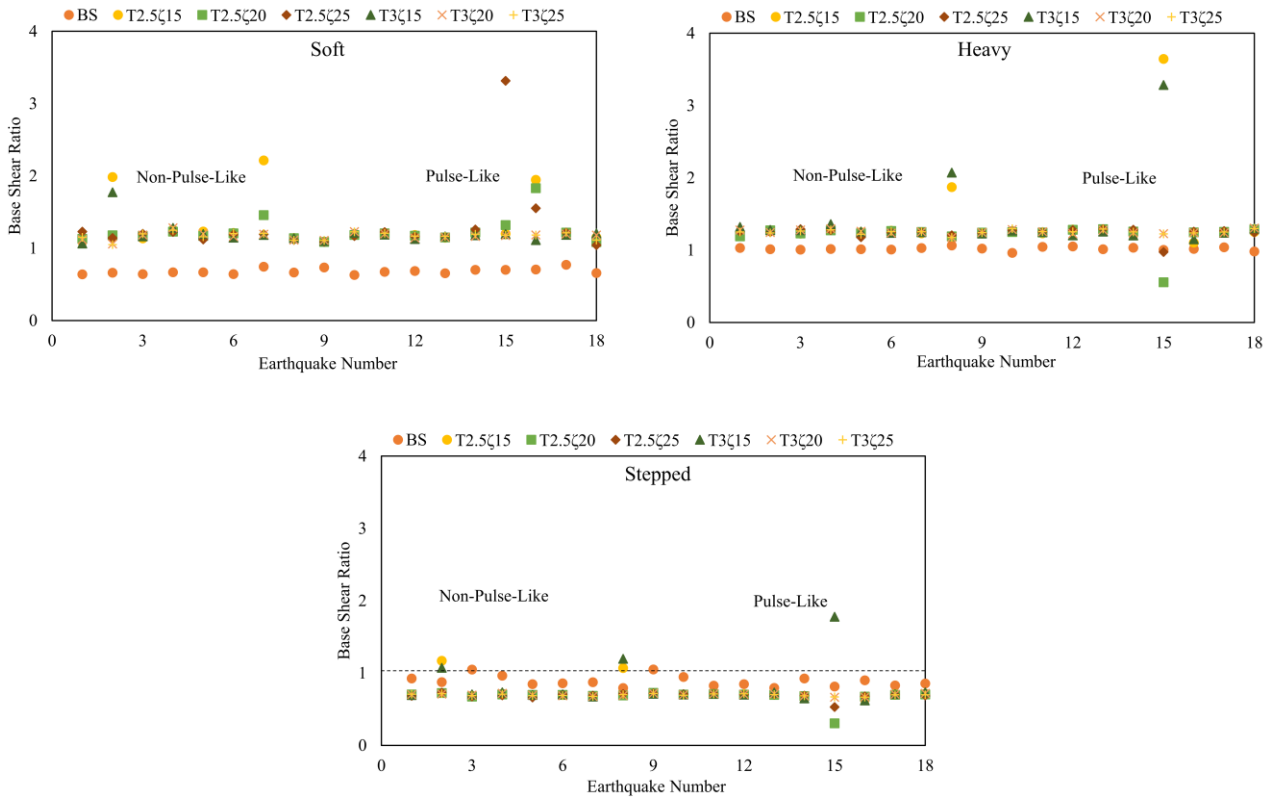

Figure 13. Roof acceleration ratio of the selected earthquakes for irregular structures (a) soft, (b) heavy, (c) stepped

Stepped structure irregularity was seen to express the highest normalized input energy results for the investigated structures, as illustrated in Figure 14. The combination with the highest value in input energy was at 2.5 seconds period and a damping ratio of 15%. On the other hand, soft structure irregularity reflected the lowest normalized input energy results among all cases. The least value in input energy was observed for the combination at 3 seconds period and a damping ratio of 15%. Although all input energy results are comparable for all combinations and cases, the input energy results at 2.5 seconds were higher compared to the results at 3 seconds.

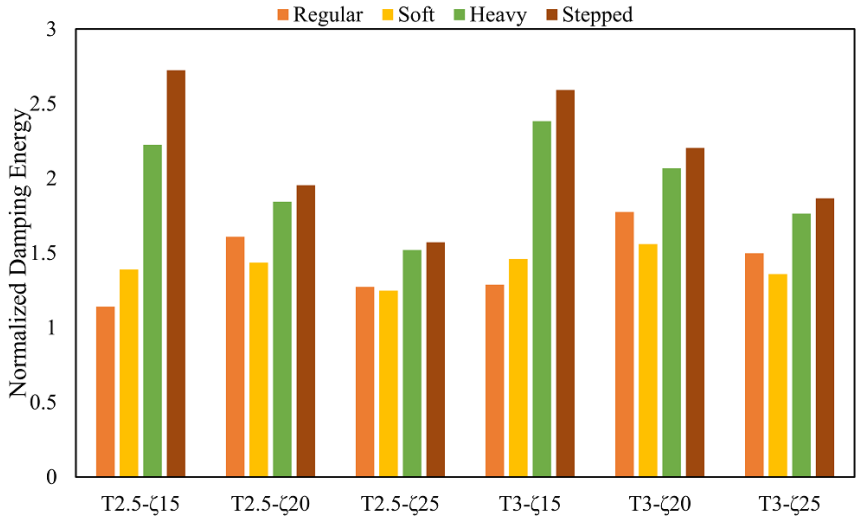

Figure 14. Normalized input energy of the investigated structures

The highest normalized input energy results for both pulse-like and non-pulse-like earthquakes were in the case of stepped structure irregularity, as shown in Figure 15. Soft story irregularity exhibited the least normalized input energy results for pulse-like and non-pulse-like earthquakes. The input energy results under pulse-like earthquakes showed much higher values than in non-pulse-like earthquakes.

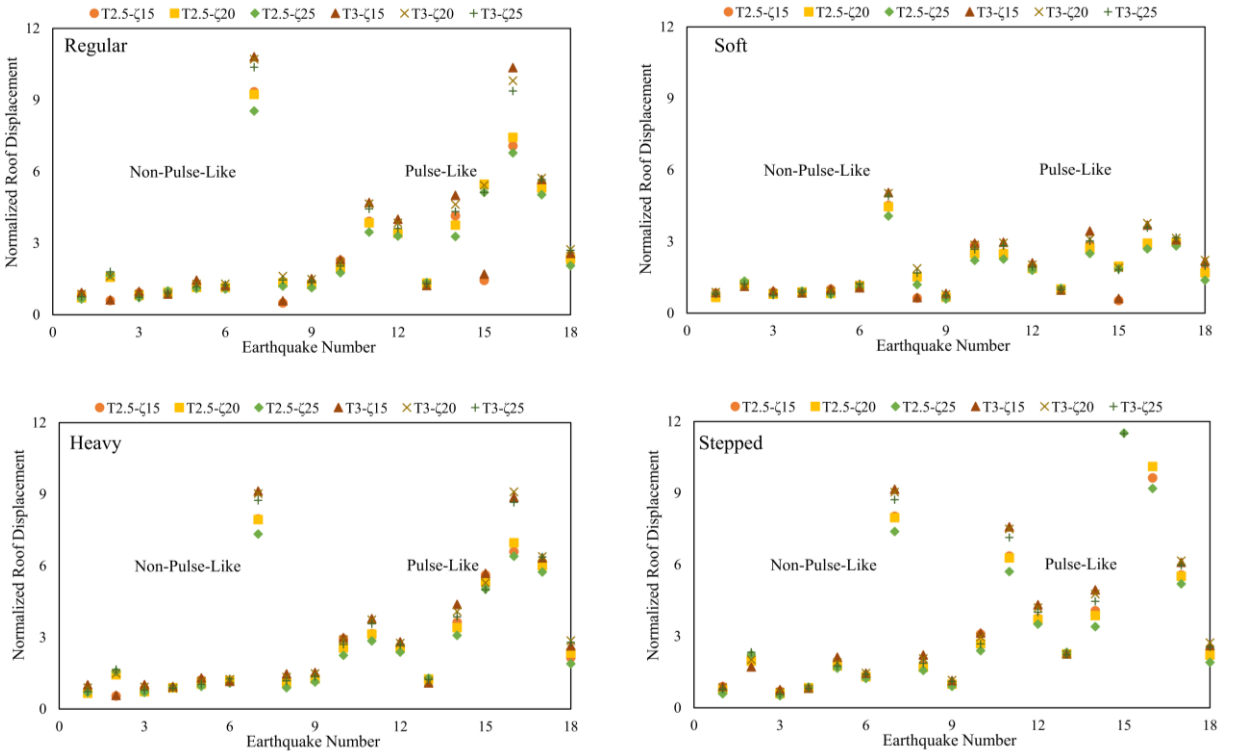

Figure 15. Normalized input energy of the selected earthquakes for (a) regular, (b) soft, (c) heavy, (d) stepped

The efficiency of the base isolator device on the behavior of different irregular structures is shown in Figure 16, where the structures utilized with the base isolator experienced better performance in input energy than bare structures. In fact, the performance of the friction pendulum isolator in the behavior of irregular structures was comparable for all combinations and cases.

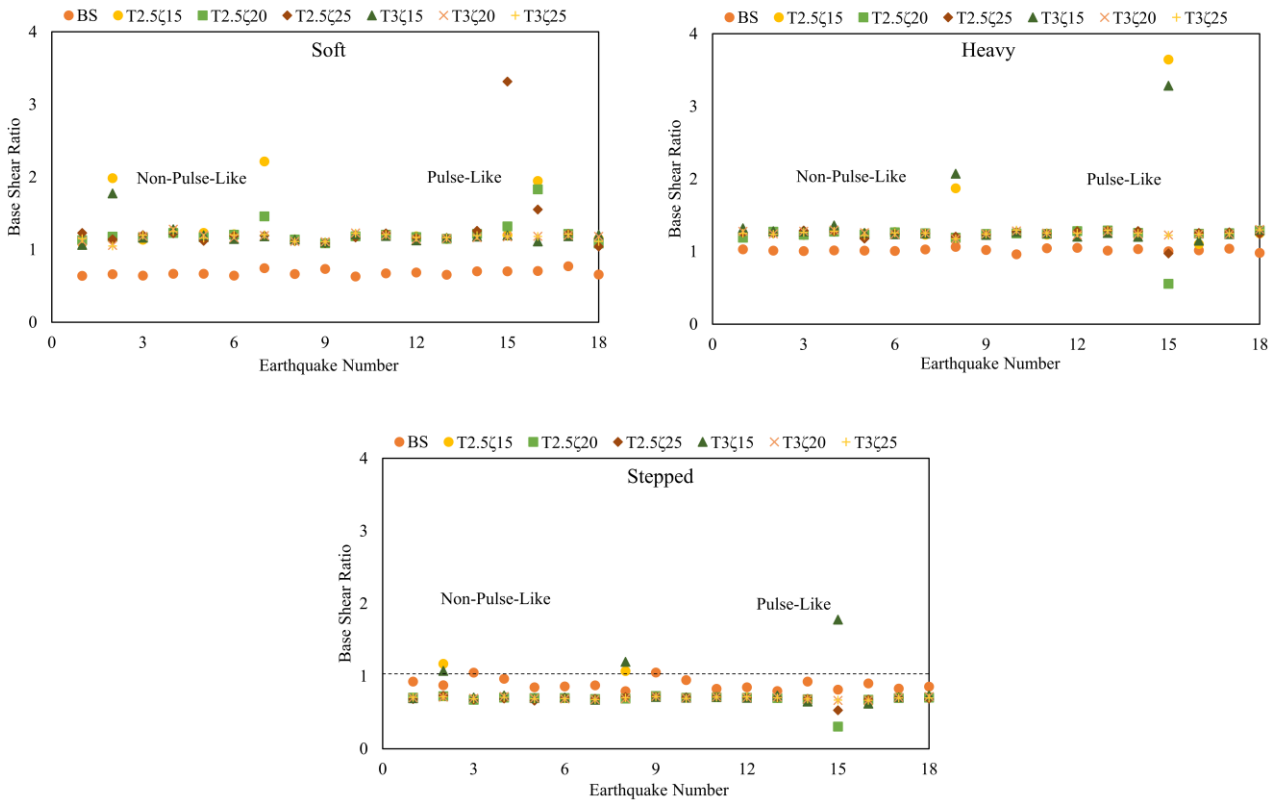

Figure 16. Input energy ratio of the selected earthquakes for irregular structures (a) soft, (b) heavy, (c) stepped

The lowest normalized damping energy value was seen in the case of regular structure for the combination of 2.5 seconds period and a 15% damping ratio, as shown in Figure 17. Nonetheless, the normalized damping energy results for regular and soft structures were very similar in terms of low values. The stepped structure case showed the highest damping energy values for all cases and combinations, where the highest value was observed at 2.5 seconds period and a 15% damping ratio. Lastly, damping energy results at the period of 3 seconds were higher for all causes compared to the period of 2.5 seconds.

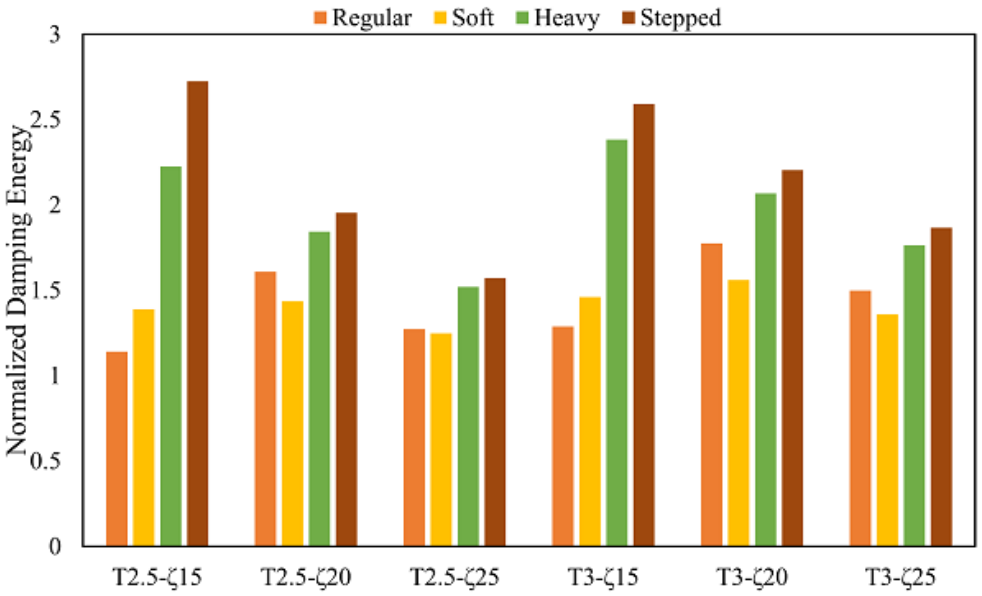

Figure 17. Normalized damping energy of the investigated structures

The highest normalized damping energy results for pulse-like and non-pulse-like earthquakes were recorded for stepped structure irregularity, as shown in Figure 18. Regular and soft structures expressed the lowest damping energy, and Pulse-like earthquakes reflected higher damping energy values in contrast to non-pulse-like earthquakes.

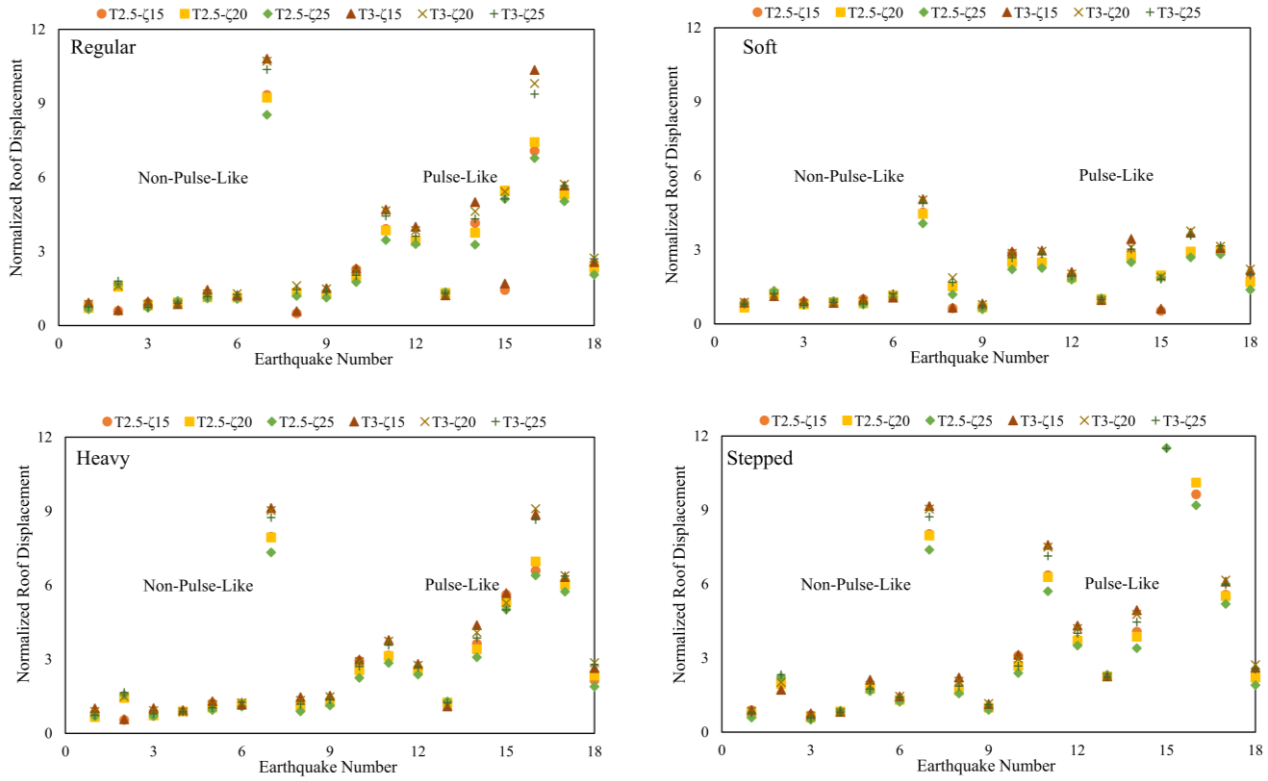

Figure 18. Normalized damping energy of the selected earthquakes for (a) regular, (b) soft, (c) heavy, (d) stepped

The friction pendulum isolator is proved to be highly efficient in the behavior of different irregular structures in terms of damping energy, as illustrated in Figure 19. The performance of the base isolator on the damping energy response is similar for all irregular cases.

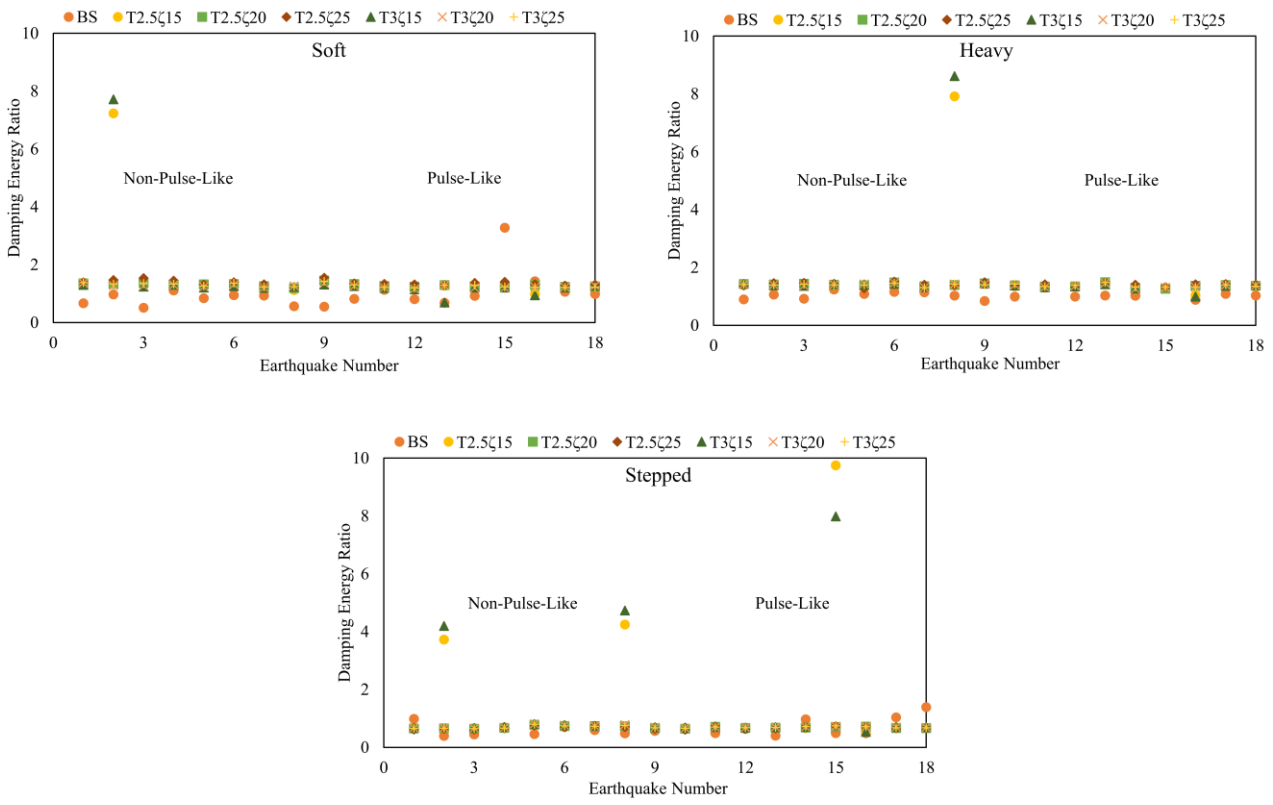

Figure 19. Normalized damping energy of the selected earthquakes for irregular structures (a) soft, (b) heavy, (c) stepped

Soft structure irregularity showed the lowest normalized hysteretic energy, where the least value was marked for the combination of 3 seconds period and a 15% damping ratio, as illustrated in Figure 20. On the contrary, stepped structure irregularity reflected the highest hysteretic energy results, where the highest value was observed for the combination of 2.5 seconds period and a 25% damping ratio. The lowest hysteretic energy value among all combinations and cases was recorded at 3 seconds period and 15% damping ratio, while the highest hysteretic energy value among all combinations and cases was seen at 2.5 seconds period and 25% damping ratio. Lastly, the normalized hysteretic energy results at 2.5 seconds showed higher values with respect to the hysteretic energy results at 3 seconds.

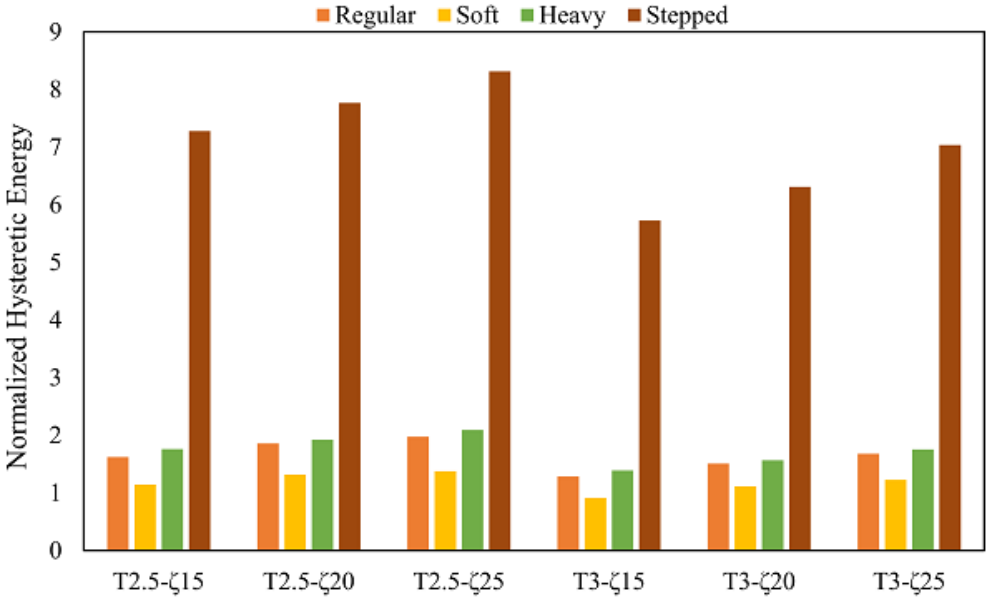

Figure 20. Normalized hysteretic energy of the investigated structures

Normalized hysteretic energy results for pulse-like and non-pulse-like earthquakes were reported as the highest value for the case of the stepped structure, while soft structure irregularity represented the lowest value, as shown in Figure 21. Generally, pulse-like earthquakes exhibited higher hysteretic energy values compared to non-pulse-like earthquakes.

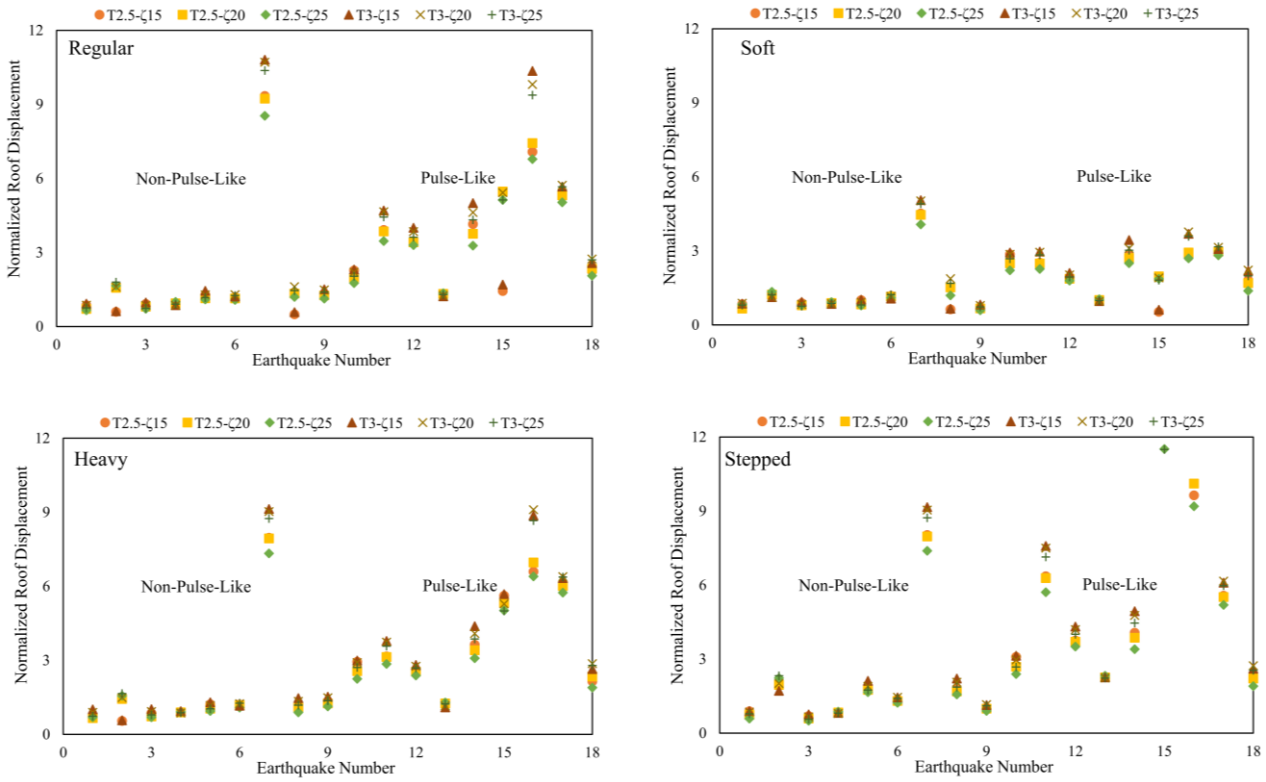

Figure 21. Normalized hysteretic energy of the selected earthquakes for (a) regular, (b) soft, (c) heavy, (d) stepped

Stepped structure irregularity experienced the best performance of friction pendulum isolator in terms of hysteretic energy, as illustrated in Figure 22. On the other hand, soft structure irregularity exhibited the lowest performance of friction pendulum isolator where the values of soft bare structure exceeded that of the base-isolated soft structure.

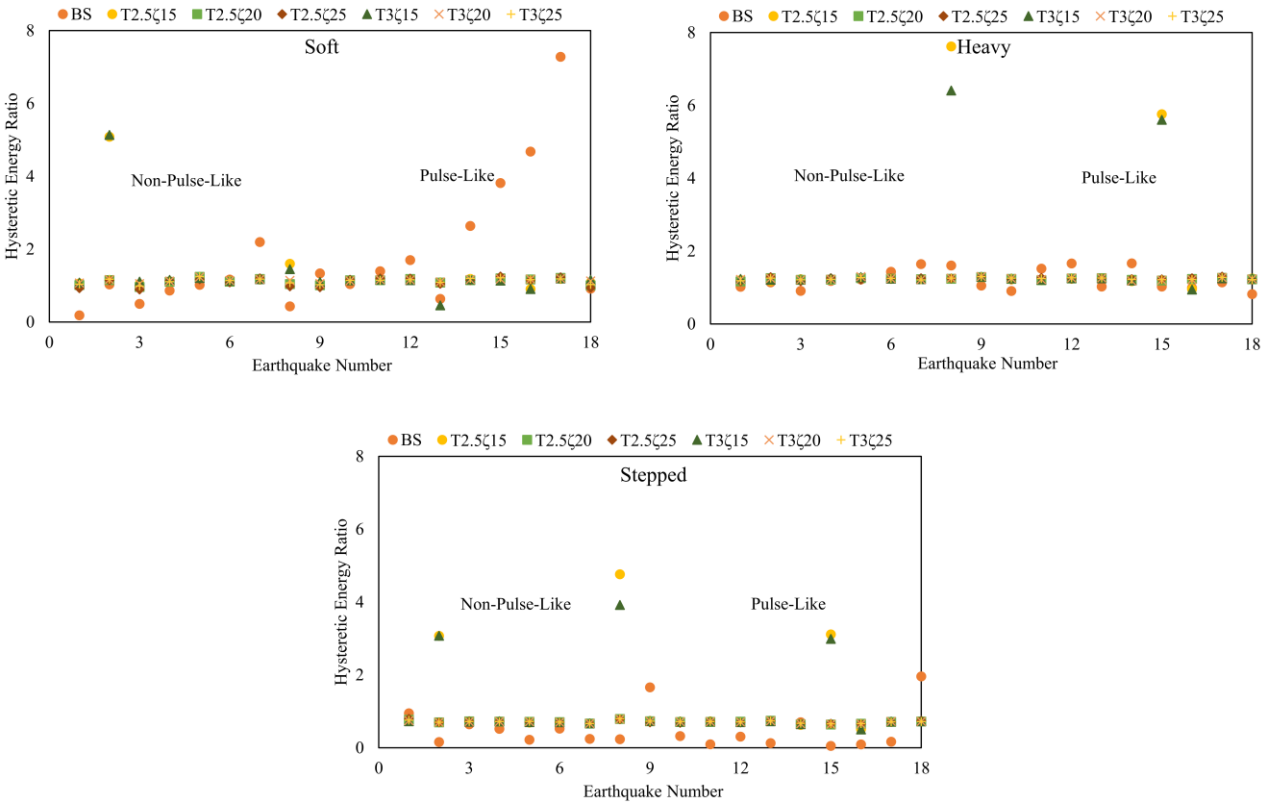

Figure 22. Normalized hysteretic energy of the selected earthquakes for irregular structures (a) soft, (b) heavy, (c) stepped

In order to investigate the influence of pulse-like and non-pulse-like earthquakes on the efficiency and performance of the friction pendulum isolator, two earthquake records with similar PGA, PGA/PGV ratio, soil type, and earthquake magnitude were selected in order to neutralize the effect of these earthquake characteristics and solely evaluate the effect of non-pulse-like record (RSN 6) and pulse-like record (RSN 159).

The hysteresis loop is considered highly crucial in the analysis and design of structures by means of seismic performance due to the fact that the hysteresis loop reflects the damage in relation to linear and nonlinear properties. The largest loop cycle in the friction pendulum isolator was observed in heavy story irregularity, as illustrated in Figure 23. On the other hand, stepped structure irregularity displayed the smallest loop cycle. The combination of 2.5 seconds period and 25% damping ratio represented the most extensive loop cycle, while the combination of 3 seconds period and 15% damping ratio showed the minor loop cycle.

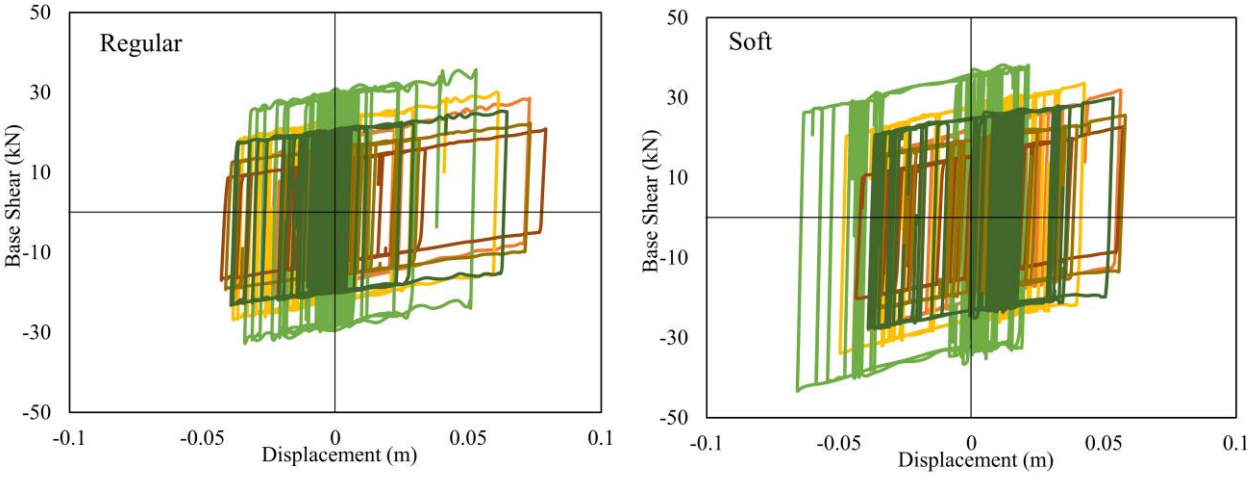

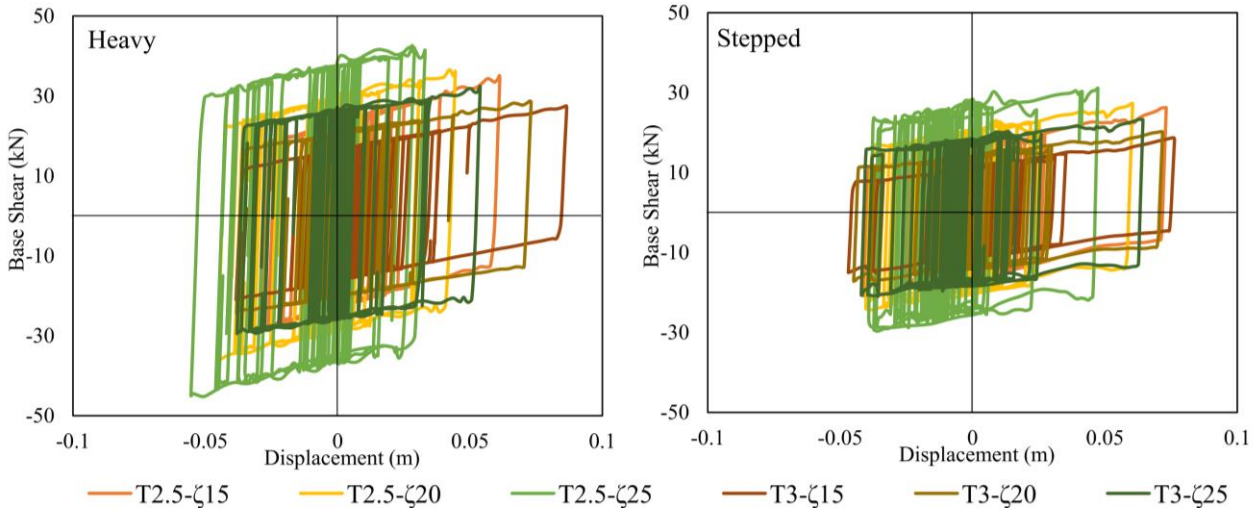

Figure 23. Behavior of the friction pendulum bearings under non-pulse-like earthquake (RSN 6)

Heavy story case showed the most significant loop cycle in friction pendulum isolator as represented in Figure 24. The smallest loop cycle was observed in the case of the stepped structure. Among all combinations and all cases, the combination of 2.5 seconds period and 25% damping ratio exhibited the largest loop cycle, while the combination of 3 seconds period and 15% damping ratio displayed the smallest loop cycle.

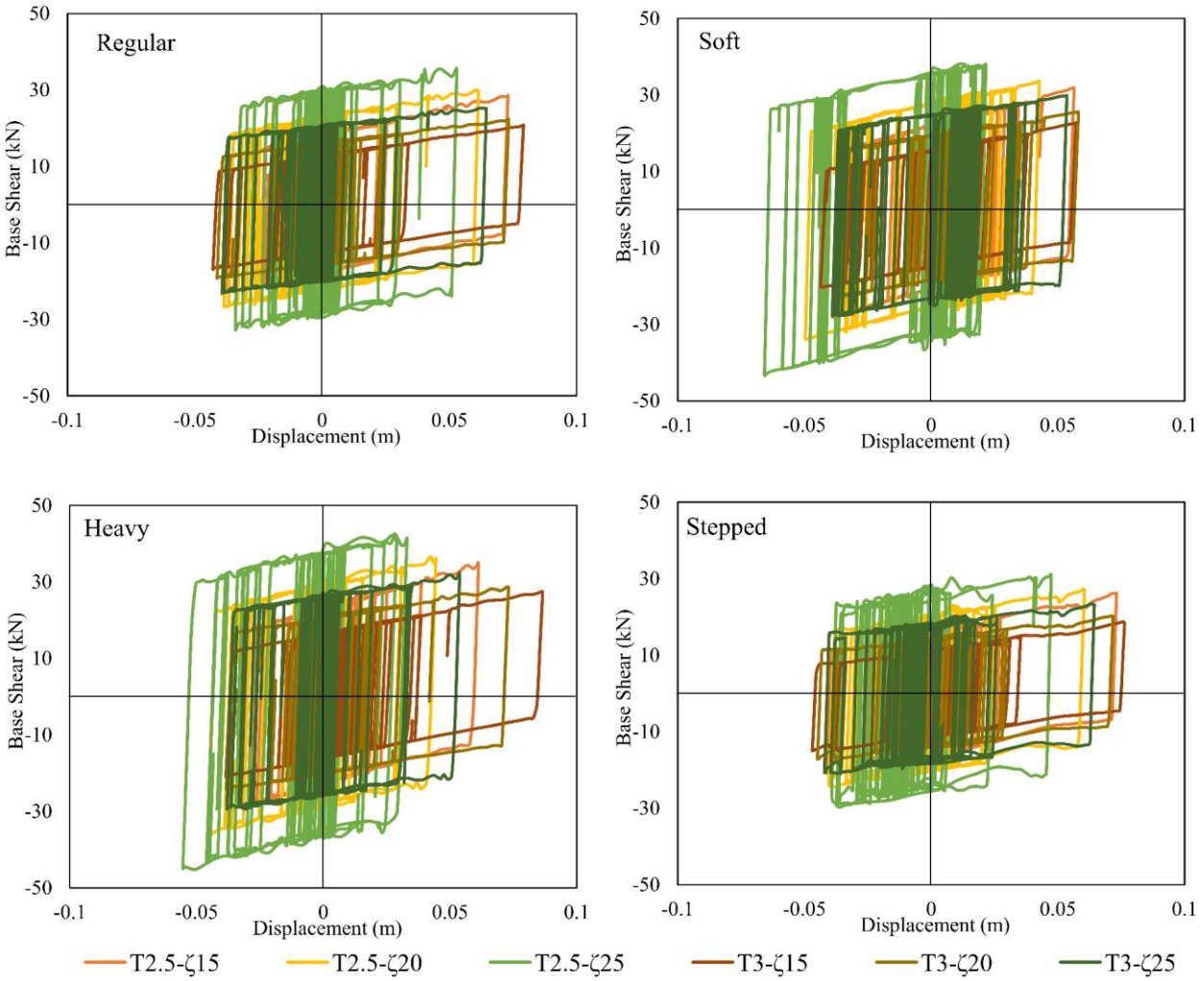

Figure 24. Behavior of the friction pendulum bearings under pulse-like earthquake (RSN 159)

This section is devoted to investigating the effect of earthquake characteristics on the performance of friction pendulum isolators using statistical analysis where the earthquake characteristics (fault distance, arias intensity, etc.), isolator properties (damping ratio, period), and structure type (regular, soft, etc.) were selected to perform the analysis. The severity of an earthquake is generally determined by several factors such as fault distance and arias intensity. Thus,

correlation coefficient (R) or Pearson's correlation coefficient and bivariate correlation were conducted to determine the significant factors correlated with the investigated response by analyzing the intensity of the linear relation between the earthquake factors and the corresponding structural response. The extremes of the correlation coefficient are -1 and +1, where the value near these two represents a strong linear association, as stated by Asuero et al. [31]. The significance value (P-value) was computed for each structural response (base shear, roof displacement, etc.) in relation to each earthquake factor (fault distance, arias intensity, etc.) in order to indicate the significance where the P-value was lower than or equal of 0.05 is taken into account as significant and values bigger than 0.05 is considered insignificant.

The significance of each structural response (base shear, roof displacement, etc.) differs depending on the type of structure (regular, soft, etc.), as illustrated in Table 2. However, the independent parameters which exhibit the significance of base shear response are PGV, PGD, PGA/PGV, T5, T75, SV, and SD. Regarding roof displacement, the significant parameters are PGV, PGD, PGA/PGV, T5, T75, D5-75, T95, SV, and SD. Finally, the common significant parameters between base shear and roof displacement responses are PGV, PGD, PGA/PGV, T5, T75, SV, and SD.

Table 2. Influence of earthquake properties on the base shear and roof displacement

Parameters	Base Shear								Roof Displacement							
	Regular		Soft		Heavy		Stepped		Regular		Soft		Heavy		Stepped	
	R	P-Value	R	P-Value	R	P-Value	R	P-Value	R	P-Value	R	P-Value	R	P-Value	R	P-Value
R_{rup}	-0.166	0.086	-0.114	0.239	-0.195	0.043	-0.109	0.261	-0.175	0.07	-0.184	0.056	-0.201	0.037	-0.154	0.112
Vs30	0.003	0.974	-0.041	0.674	-0.01	0.919	-0.094	0.332	0.168	0.083	0.087	0.37	0.121	0.212	-0.077	0.429
PGA	-0.103	0.288	-0.125	0.197	-0.118	0.224	-0.038	0.693	-0.93	0.339	-0.031	0.748	-0.037	0.705	-0.085	0.38
PGV	0.508	0	0.423	0	0.58	0	0.515	0	0.476	0	0.435	0	0.602	0	0.651	0
PGD	0.698	0	0.571	0	0.803	0	0.558	0	0.826	0	0.777	0	0.838	0	0.76	0
PGA/PGV	-0.664	0	-0.564	0	-0.764	0	-0.551	0	-0.686	0	-0.66	0	-0.737	0	-0.761	0
AI	-0.015	0.878	-0.068	0.482	-0.015	0.881	-0.004	0.968	0.078	0.425	0.148	0.125	0.148	0.127	-0.031	0.749
T5	0.399	0	0.317	0.001	0.461	0	0.242	0.012	0.592	0	0.513	0	0.577	0	0.392	0
T75	0.365	0	0.295	0.002	0.422	0	0.197	0.041	0.565	0	0.49	0	0.533	0	0.336	0
D5-75	0.25	0.009	0.211	0.028	0.289	0.002	0.091	0.349	0.431	0	0.373	0	0.375	0	0.19	0.049
T95	0.291	0.002	0.239	0.013	0.338	0	0.149	0.124	0.483	0	0.422	0	0.438	0	0.256	0.007
D5-95	0.106	0.276	0.099	0.309	0.126	0.192	0.012	0.902	0.255	0.008	0.227	0.018	0.187	0.053	0.048	0.62
SV	0.416	0	0.333	0	0.473	0	0.394	0	0.432	0	0.398	0	0.528	0	0.512	0
SD	0.617	0	0.524	0	0.708	0	0.474	0	0.678	0	0.571	0	0.718	0	0.684	0
STD	0.028	0.776	-0.001	0.99	0.033	0.738	0.064	0.512	0.012	0.9	0.08	0.413	0.086	0.378	0.04	0.684
EQ-D	-0.049	0.611	-0.051	0.598	-0.045	0.644	-0.041	0.672	0.033	0.734	0.068	0.482	0.016	0.868	-0.057	0.557

Roof acceleration response reflected no significant constant parameters among the structure types where soft structure irregularity had one significant parameter, which is Vs30, while the rest of the structures showed significance in PGV, PGD, PGA/PGV, SV, and SD as represented in Table 3. On the other hand, input energy response expressed significance in the following parameters: PGV, PGD, PGA/PGV, SV, and SD. The common significant parameters among roof acceleration (excluding soft story) and input energy are PGV, PGD, PGA/PGV, SV, and SD.

Table 3. Influence of earthquake properties on the roof acceleration and input energy

Parameters	Base Shear								Roof Displacement							
	Regular		Soft		Heavy		Stepped		Regular		Soft		Heavy		Stepped	
	R	P-Value	R	P-Value	R	P-Value	R	P-Value	R	P-Value	R	P-Value	R	P-Value	R	P-Value
R_{rup}	-0.121	0.212	-0.139	0.15	0.034	0.728	-0.014	0.885	-0.208	0.031	-0.212	0.027	-0.204	0.034	-0.087	0.373
Vs30	-0.022	0.822	-0.181	0.06	-0.073	0.45	-0.202	0.036	0.123	0.203	-0.003	0.976	0	0.999	-0.216	0.025
PGA	0.102	0.291	-0.099	0.306	-0.038	0.699	0.004	0.963	0.108	0.264	-0.018	0.854	0.096	0.323	-0.053	0.589
PGV	0.169	0.081	0.042	0.663	0.189	0.05	0.307	0.001	0.705	0	0.421	0	0.767	0	0.645	0
PGD	0.342	0	0.066	0.499	0.33	0	0.161	0.097	0.745	0	0.691	0	0.685	0	0.54	0
PGA/PGV	-0.269	0.005	-0.079	0.415	-0.301	0.002	0-.278	0.004	-0.684	0	-0.588	0	-0.69	0	-0.603	0
AI	0.158	0.102	-0.096	0.322	0.04	0.68	-0.18	0.856	0.216	0.025	0.085	0.382	0.179	0.064	-0.099	0.309
T5	0.345	0	0.003	0.976	0.261	0.006	-0.074	0.445	0.378	0	0.269	0.005	0.318	0.001	0.101	0.299
T75	0.329	0.001	0.056	0.567	0.281	0.003	-0.081	0.404	0.315	0.001	0.266	0.005	0.243	0.011	0.043	0.658

D5-75	0.25	0.009	0.134	0.166	0.27	0.005	-0.079	0.414	0.161	0.095	0.219	0.023	0.081	0.404	-0.06	0.54
T95	0.317	0.001	0.072	0.461	0.275	0.004	-0.084	0.39	0.207	0.032	0.214	0.026	0.134	0.166	-0.002	0.98
D5-95	0.216	0.025	0.132	0.172	0.229	0.017	-0.075	0.438	-0.03	0.762	0.105	0.279	-0.1	0.302	-0.117	0.228
SV	0.17	0.079	0.044	0.648	0.185	0.056	0.226	0.019	0.657	0	0.415	0	0.672	0	0.457	0
SD	0.3	0.002	0.014	0.889	0.384	0	0.198	0.04	0.701	0	0.489	0	0.707	0	0.472	0
STD	0.041	0.671	-0.003	0.977	0.006	0.951	0.117	0.229	0.251	0.009	0.135	0.163	0.239	0.013	0.086	0.378
EQ-D	0.342	0	-0.136	0.16	0.187	0.053	-0.118	0.222	-0.088	0.363	-0.048	0.625	-0.103	0.289	-0.152	0.116

Table 4. Influence of earthquake properties on the damping energy and hysteretic energy

Parameters	Base Shear								Roof Displacement							
	Regular		Soft		Heavy		Stepped		Regular		Soft		Heavy		Stepped	
	R	P-Value	R	P-Value	R	P-Value	R	P-Value	R	P-Value	R	P-Value	R	P-Value	R	P-Value
R_{rup}	-0.134	0.167	-0.191	0.048	-0.137	0.159	-0.059	0.543	-0.204	0.034	-0.129	0.183	-0.201	0.037	-0.137	0.159
Vs30	-0.169	0.08	0.003	0.978	-0.209	0.03	0.189	0.051	0.291	0.002	-0.433	0	0.184	0.056	0.021	0.825
PGA	0.024	0.805	0.048	0.622	0.033	0.732	-0.121	0.214	0.302	0.002	-0.112	0.249	0.28	0.003	0.173	0.074
PGV	0.603	0	0.642	0	0.667	0	0.107	0.272	0.663	0	-0.083	0.391	0.69	0	0.771	0
PGD	0.484	0	0.7	0	0.495	0	0.306	0.001	0.58	0	0.006	0.952	0.61	0	0.538	0
PGA/PGV	-0.523	0	-0.663	0	-0.544	0	-0.306	0.001	-0.495	0	-0.109	0.264	-0.502	0	-0.594	0
AI	-0.018	0.851	0.059	0.545	-0.031	0.747	-0.064	0.508	0.508	0	-0.035	0.721	0.495	0	0.269	0.005
T5	0.038	0.7	0.168	0.082	0.012	0.901	0.565	0	0.42	0	-0.05	0.608	0.399	0	0.333	0
T75	-0.017	0.861	0.117	0.228	-0.05	0.61	0.534	0	0.343	0	0.059	0.544	0.312	0.001	0.239	0.013
D5-75	-0.105	0.28	0.013	0.891	-0.144	0.137	0.398	0	0.16	0.097	0.23	0.017	0.119	0.222	0.045	0.645
T95	-0.066	0.499	0.048	0.621	-0.1	0.301	0.428	0	0.225	0.019	0.115	0.237	0.19	0.049	0.136	0.159
D5-95	-0.166	0.085	-0.096	0.321	-0.204	0.034	0.181	0.061	-0.043	0.66	0.273	0.004	-0.085	0.383	-0.113	0.245
SV	0.464	0	0.551	0	0.512	0	0.139	0.151	0.669	0	-0.052	0.595	0.654	0	0.635	0
SD	0.439	0	0.529	0	0.469	0	0.558	0	0.546	0	-0.04	0.678	0.549	0	0.552	0
STD	0.174	0.072	0.223	0.02	0.196	0.042	-0.213	0.027	0.35	0	-0.06	0.535	0.316	0.001	0.218	0.024
EQ-D	-0.172	0.075	-0.185	0.055	-0.19	0.049	0.191	0.048	-0.019	0.848	0.08	0.408	-0.008	0.937	-0.061	0.529

Finally, this study has demonstrated the influence of different irregularity types on the behavior of base-isolated structures. These results are similar to previous studies [32, 33]. Besides, the study outcomes obviously impacted various earthquake characteristics on the isolator responses. Similar observations were also discussed in the literature [34-36].

4. Conclusion

This paper has focused on evaluating the seismic performance of low-rise base-isolated RC frames under pulse-like and non-pulse-like earthquakes. Furthermore, the impact of three vertical irregularities (soft story, heavy story, and stepped structure) was studied on base-isolated RC structures' responses. The efficiency of a friction pendulum isolator equipped with different types of irregular structures under various types of earthquakes was studied compared to the reference model, which is a regular structure, and the results were reported. Based on the study's results, it was observed that the friction pendulum isolator proved its efficiency in minimizing the responses of base-isolated RC structures. The influence of vertical irregularity is highly dependent on the investigated response. Moreover, the soft story case exhibited the most drastic behavior in contrast to the other irregularity types, which is attributed to the fact that soft story irregularity arises from the increase in the structure's natural period, which leads to a decrease in the performance of the friction pendulum isolator.

The period of friction pendulum isolator significantly impacted the performance of base-isolated RC structures compared to the damping ratio, which played little to no effect. Furthermore, pulse-like earthquakes reflected more severe behavior on the efficiency of the friction pendulum isolator utilized with RC structures compared to non-pulse-like earthquakes. The significant constant parameters among all structural responses (base shear, roof displacement, etc.) were PGD, PGA/PGV, and SD. Further efforts are still needed in this field to evaluate the performance of generations of friction pendulum bearings and to study the friction pendulum's capability under the combined effects of vertical and horizontal ground motions with pulse characteristics. Besides, it is recommended to come up with some design factors of safety to account for the effects of pulse-like ground motions.

5. List of Nomenclature

Abbreviation	Definition	Unit
BS	Bare structure	-
MSE	Mean square of error	Squared of the response's unit itself
Q_d	Horizontal strength	kN
μ	Sliding coefficient of friction	-
W	Weight of the superstructure	kN
K_d	Second-slope stiffness	kN/m
r	Radius of curvature of the spherical concave dish	m
T_d	Period of isolator	s
g	Acceleration due to gravity	m/s^2
R	Coefficient of correlation	-
RC	Reinforced concrete	-
R_{Rup}	Closest distance to the rupture plane	km
AI	Arias Intensity	m/sec
T5	time at which 5% of the arias intensity has occurred	s
T75	time at which 75% of the arias intensity has occurred	s
T95	time at which 95% of the arias intensity has occurred	s
D5-75	Duration between 5% and 75% of the arias intensity	s
D5-95	Duration between 5% and 95% of the arias intensity	s
SV	Spectral velocity	m/s
SD	Spectral displacement	m
STD	Standard deviation of the acceleration time history	g
PGA	Peak ground acceleration	g
PGV	Peak ground velocity	m/s
PGD	Peak ground displacement	m
PGA/PGV	Peak ground acceleration/Peak ground velocity	g/m/s
Vs30	The time-averaged shear wave velocity to 30 meters depth	m/s
EQ-D	Duration of the earthquake	s

6. Declarations

6.1. Author Contributions

Conceptualization, J.A., S.K., and J.T.; methodology, J.A., S.K., and B.Y.; formal analysis, S.K. and J.T.; investigation, J.A. writing—original draft preparation, J.A. and S.K.; writing—review and editing, J.T., B.Y., and Y.A.; visualization, Y.A.; All authors have read and agreed to the published version of the manuscript.

6.2. Data Availability Statement

The data presented in this study are available on request from the corresponding author.

6.3. Funding

The authors received no financial support for the research, authorship, and/or publication of this article.

6.4. Conflicts of Interest

The authors declare no conflict of interest.

7. References

[1] Sarkar, P., Prasad, A. M., & Menon, D. (2010). Vertical geometric irregularity in stepped building frames. Engineering Structures, 32(8), 2175–2182. doi:10.1016/j.engstruct.2010.03.020.

[2] Inel, M., Ozmen, H. B., & Bilgin, H. (2008). Re-evaluation of building damage during recent earthquakes in Turkey. Engineering Structures, 30(2), 412–427. doi:10.1016/j.engstruct.2007.04.012.

[3] Kim, S. J., & Elnashai, A. S. (2009). Characterization of shaking intensity distribution and seismic assessment of RC buildings for the Kashmir (Pakistan) earthquake of October 2005. Engineering Structures, 31(12), 2998–3015. doi:10.1016/j.engstruct.2009.08.001.

[4] Varadharajan, S., Sehgal, V. K., & Saini, B. (2012). Review of different structural irregularities in buildings. Journal of Structural Engineering (India), 39(5), 538–563.

[5] Parulekar, Y. M., & Reddy, G. R. (2009). Passive response control systems for seismic response reduction: A state-of-the-art review. International Journal of Structural Stability and Dynamics, 9(1), 151–177. doi:10.1142/S0219455409002965.

[6] Kangda, M. Z., & Bakre, S. (2018). The Effect of LRB Parameters on Structural Responses for Blast and Seismic Loads. Arabian Journal for Science and Engineering, 43(4), 1761–1776. doi:10.1007/s13369-017-2732-7.

[7] Rong, Q. (2020). Optimum parameters of a five-story building supported by lead-rubber bearings under near-fault ground motions. Journal of Low Frequency Noise Vibration and Active Control, 39(1), 98–113. doi:10.1177/1461348419845829.

[8] Mazza, F., & Labernarda, R. (2018). Effects of nonlinear modelling of the base-isolation system on the seismic analysis of R.C. buildings. Procedia Structural Integrity, 11, 226–233. doi:10.1016/j.prostr.2018.11.030.

[9] Hall, J. F., Heaton, T. H., Halling, M. W., & Wald, D. J. (1995). Near-Source Ground Motion and its Effects on Flexible Buildings. Earthquake Spectra, 11(4), 569–605. doi:10.1193/1.1585828.

[10] Mazza, F., & Vulcano, A. (2012). Effects of near-fault ground motions on the nonlinear dynamic response of base-isolated R.C. framed buildings. Earthquake Engineering and Structural Dynamics, 41(2), 211–232. doi:10.1002/eqe.1126.

[11] Mazza, F., & Mazza, M. (2016). Nonlinear seismic analysis of irregular R.C. framed buildings base-isolated with friction pendulum system under near-fault excitations. Soil Dynamics and Earthquake Engineering, 90, 299–312. doi:10.1016/j.soildyn.2016.08.028.

[12] Jangid, R. S., & Kelly, J. M. (2001). Base isolation for near-fault motions. Earthquake Engineering and Structural Dynamics, 30(5), 691–707. doi:10.1002/eqe.31.

[13] Mazza, F. (2018). Seismic demand of base-isolated irregular structures subjected to pulse-type earthquakes. Soil Dynamics and Earthquake Engineering, 108, 111–129. doi:10.1016/j.soildyn.2017.11.030.

[14] Mazza, F., Mazza, M., & Vulcano, A. (2018). Base-isolation systems for the seismic retrofitting of R.C. framed buildings with soft-storey subjected to near-fault earthquakes. Soil Dynamics and Earthquake Engineering, 109, 209–221. doi:10.1016/j.soildyn.2018.02.025.

[15] Sadashiva, V. K., MacRae, G. A., & Deam, B. L. (2009). Determination of structural irregularity limits - Mass irregularity example. Bulletin of the New Zealand Society for Earthquake Engineering, 42(4), 288–301. doi:10.5459/bnzsee.42.4.288-301.

[16] Michalis, F., Dimitrios, V., & Manolis, P. (2006). Evaluation of the influence of vertical irregularities on the seismic performance of a nine-storey steel frame. Earthquake Engineering & Structural Dynamics, 35(12), 1489–1509. doi:10.1002/eqe.591.

[17] ASCE/SEI 7-16. (2016). Minimum Design Loads For Buildings and Other Structures. American Society of Civil Engineering (ASCE), Reston, United States.

[18] Ghosh, R., & Debbarma, R. (2017). Performance evaluation of setback buildings with open ground storey on plain and sloping ground under earthquake loadings and mitigation of failure. International Journal of Advanced Structural Engineering, 9(2), 97–110. doi:10.1007/s40091-017-0151-3.

[19] Warn, G. P., & Ryan, K. L. (2012). A review of seismic isolation for buildings: Historical development and research needs. Buildings, 2(3), 300–325. doi:10.3390/buildings2030300.

[20] Constantinou, M., Mokha, A., & Reinhorn, A. (1990). Teflon Bearings in Base Isolation II: Modeling. Journal of Structural Engineering, 116(2), 455–474. doi:10.1061/(asce)0733-9445(1990)116:2(455).

[21] ACI committee 318-19. (2019). Building Code Requirements for Structural Concrete and Commentary. American Concrete Institute (ACI), Farmington Hills, United States.

[22] Applied Technology Council (ATC). (2017). Guidelines for Nonlinear Structural Analysis for Design of Buildings Part IIb–Reinforced Concrete Moment Frames. Applied Technology Council (ATC), Redwood, United States. doi:10.6028/NIST.GCR.17-917-46v2.

[23] Mander, J. B., Priestley, M. J. N., & Park, R. (1988). Theoretical Stress-Strain Model for Confined Concrete. Journal of Structural Engineering, 114(8), 1804–1826. doi:10.1061/(asce)0733-9445(1988)114:8(1804).

[24] Park, R., & Paulay, T. (1991). Reinforced concrete structures. John Wiley & Sons, Hoboken, United States.

[25] Kalantari, A., & Roohbakhsh, H. (2020). Expected seismic fragility of code-conforming RC moment resisting frames under twin seismic events. Journal of Building Engineering, 28, 101098. doi:10.1016/j.jobe.2019.101098.

[26] CSI. SAP2000 - Structural Software for Analysis and Design. Computers and Structures Inc., California, United States.

[27] Kitayama, S., & Constantinou, M. C. (2018). Seismic Performance of Buildings with Viscous Damping Systems Designed by the Procedures of ASCE/SEI 7-16. Journal of Structural Engineering, 144(6), 4018050. doi:10.1061/(asce)st.1943-541x.0002048.

[28] FEMA 451B. (2007). NEHRP Recommended Provisions for Seismic Regulations for New Buildings and Other Structures: Training and Instructional Materials. Federal Emergency Management Agency (FEMA), Washington, United States.

[29] Barmo, A., Mualla, I. H., & Hasan, H. T. (2015). The Behavior of Multi-Story Buildings Seismically Isolated System Hybrid Isolation (Friction, Rubber and with the Addition of Rotational Friction Dampers). Open Journal of Earthquake Research, 04(01), 1–13. doi:10.4236/ojer.2015.41001.

[30] Chen, X., & Xiong, J. (2022). Seismic resilient design with base isolation device using friction pendulum bearing and viscous damper. Soil Dynamics and Earthquake Engineering, 153, 107073. doi:10.1016/j.soildyn.2021.107073.

[31] Asuero, A. G., Sayago, A., & González, A. G. (2006). The correlation coefficient: An overview. Critical Reviews in Analytical Chemistry, 36(1), 41–59. doi:10.1080/10408340500526766.

[32] Li, C., Chang, K., Cao, L., & Huang, Y. (2021). Performance of a nonlinear hybrid base isolation system under the ground motions. Soil Dynamics and Earthquake Engineering, 143, 106589. doi:10.1016/j.soildyn.2021.106589.

[33] Pérez-Rocha, L. E., Avilés-López, J., & Tena-Colunga, A. (2021). Base isolation for mid-rise buildings in presence of soil-structure interaction. Soil Dynamics and Earthquake Engineering, 151, 106980. doi:10.1016/j.soildyn.2021.106980.

[34] Cheshmehkaboodi, N., & Guizani, L. (2021). On the influence of earthquakes and soil characteristics on seismic response and performance of isolated bridges. Arabian Journal of Geosciences, 14(5), 1–12. doi:10.1007/s12517-021-06451-6.

[35] Zhang, H., Liu, X., Li, H., & An, N. (2021). A comparative study on the effectiveness of bidirectional and tridirectional isolation systems used in large-scale single-layer lattice domes during earthquakes. Soil Dynamics and Earthquake Engineering, 141, 106488. doi:10.1016/j.soildyn.2020.106488.

[36] Usta, P. (2021). Investigation of a base-isolator system's effects on the seismic behavior of a historical structure. Buildings, 11(5), 217. doi:10.3390/buildings11050217.